Electronic Supplementary Material (ESI) for Journal of Materials Chemistry A.

Mediating the Alloying Depth to Tune the Silicon's Morphology and Lithium-Storage Performance

Qiang Ma[a], Yan Zhao[a], Yanyang Guo[a], Zhuqing Zhao[a], Hongwei Xie[a], Pengfei Xing[a], Dihua Wang[b], and Huayi Yin[a,b,c,*]

a. Key Laboratory for Ecological Metallurgy of Multimetallic Mineral of Ministry of Education, School of Metallurgy, Northeastern University, Shenyang, 110819, P. R. China.

b. School of Resource and Environmental Science, Wuhan University, Wuhan, 430072, P. R. China.

c. Key Laboratory of Data Analytics and Optimization for Smart Industry, Ministry of Education, Northeastern University, Shenyang, 110819, P. R. China.

* Corresponding author. Email: yinhuayi@whu.edu.cn (Huayi Yin)

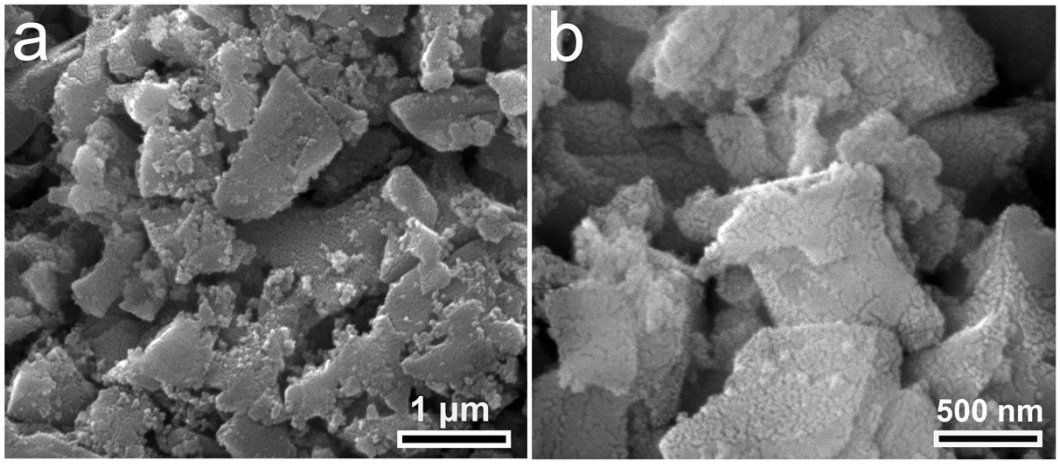

Figure S1. SEM images of the np-Si-1 sample under different magnifications.

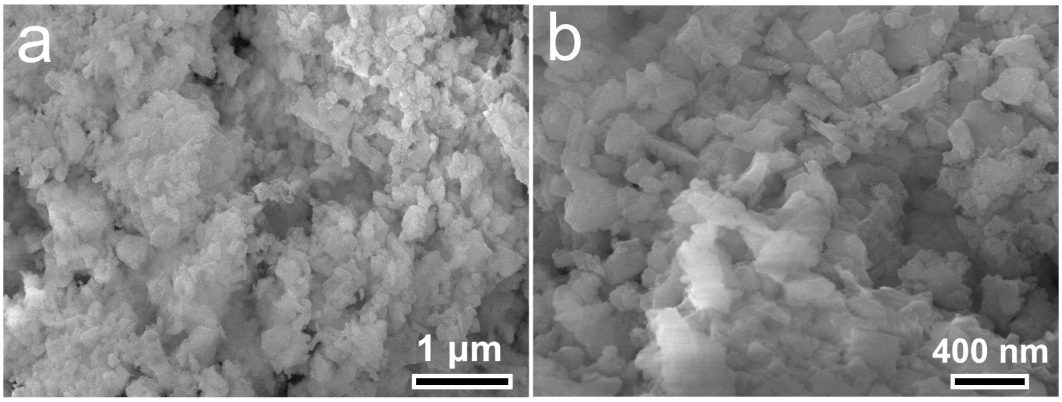

Figure S2. SEM images of the np-Si-9 sample under different magnifications.

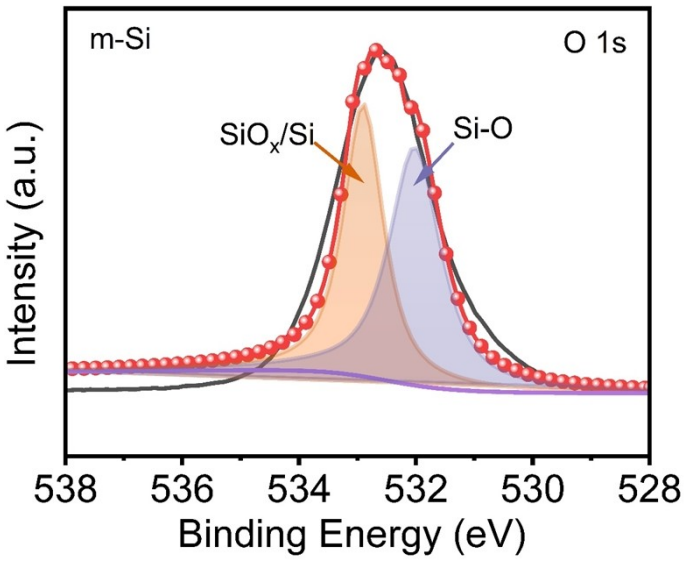

Figure S3. The high-resolution spectra of O 1s of the m-Si sample.

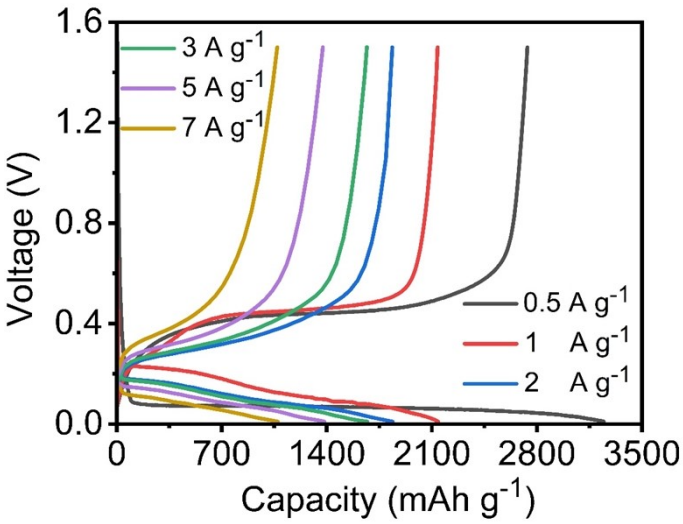

Figure S4. Galvanostatic charge/discharge voltage profiles for the np-Si-5 electrode at different current densities from 0.5 to 7 A g^{-1}.

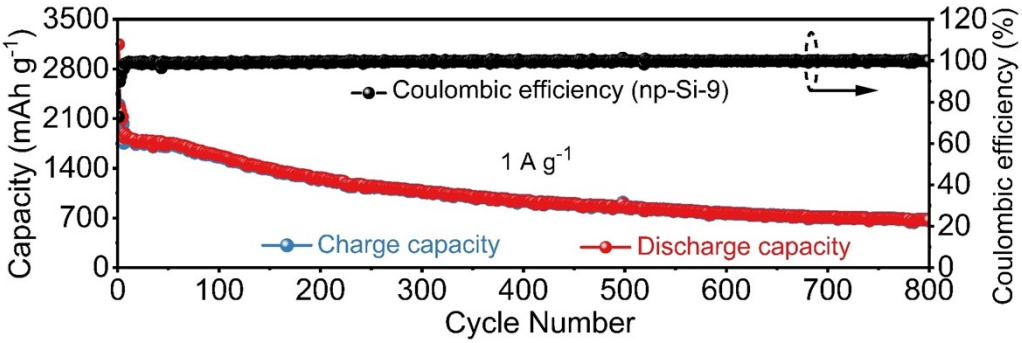

Figure S5. Long-time cycling performance and Coulombic efficiency of the np-Si-9 electrode at 1 A g^{-1} for LIBs.

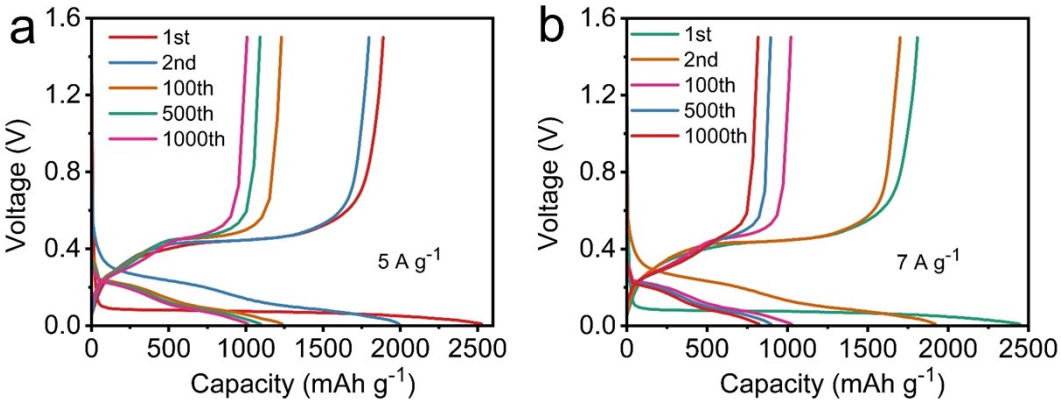

Figure S6. Galvanostatic charge/discharge voltage profiles of the np-Si-5 electrode at current densities of (a) 5 A g^{-1} and (b) 7 A g^{-1}.

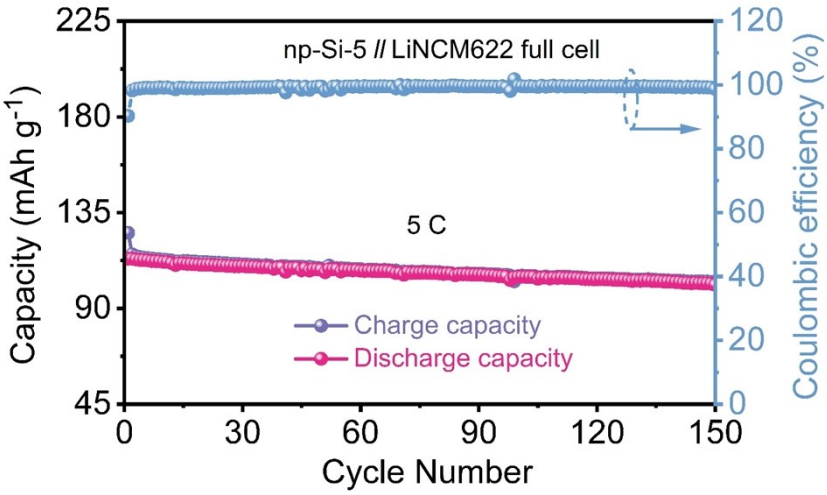

Figure S7. Cycling performance of np-Si-5//LiNCM622 full cell at 5 C for 150 cycles.

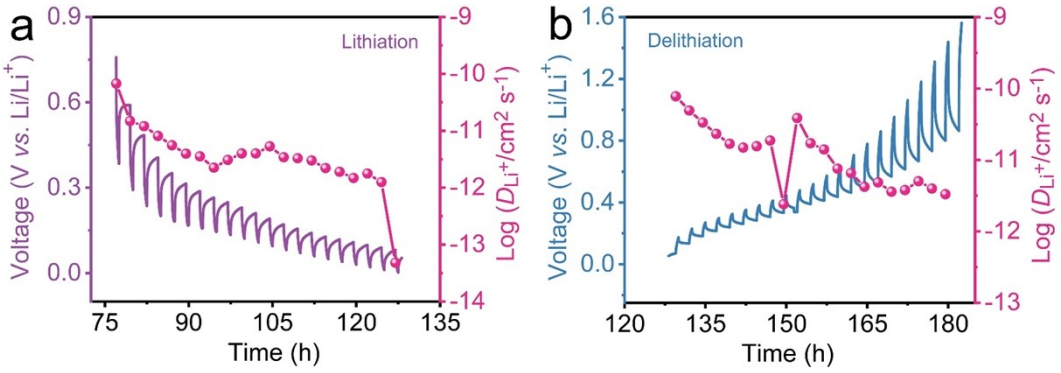

Figure S8. GITT potential profiles and corresponding D_{Li^+} of the m-Si electrode during the (a) lithiation and (b) delithiation processes.

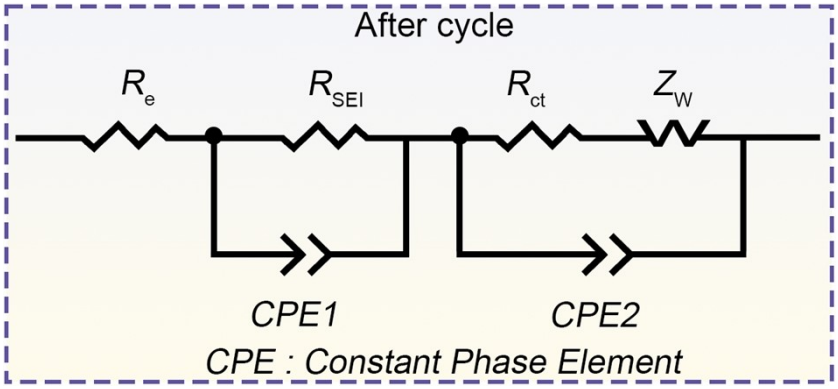

Figure S9. Equivalent circuit model of the system.

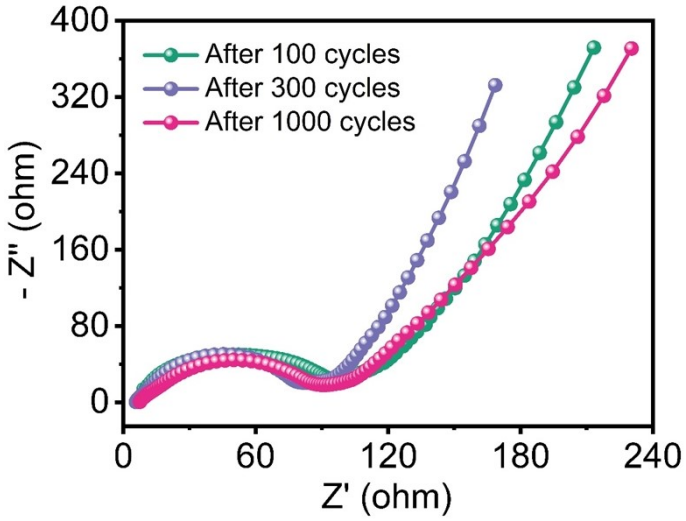

Figure S10. Nyquist plots of after 100th, 300th, and 1000th cycles of the np-Si-5 electrode.

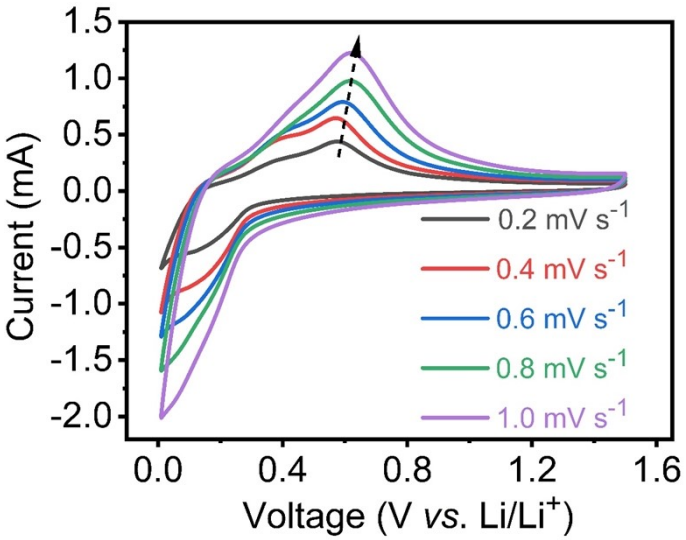

Figure S11. CV curves at different scan rates of the m-Si electrode.

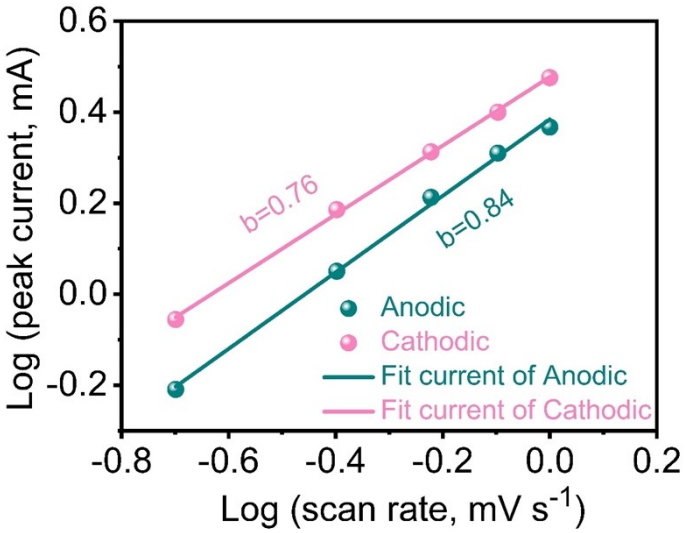

Figure S12. Determination *b*-value of the main cathodic and anodic peaks of the np-Si-5 electrode by relationship between log (peak current) and log (scan rate).

Table S1. Pore structure information for the as-made samples

Samples	BET analysis						
	S_{BET} (m^2/g)	S_{micro}[a] (m^2/g)	S_{meso}[b] (m^2/g)	V_{micro}[c] (cm^3/g)	V_{meso}[d] (cm^3/g)	D_{aver} (nm)	S_{micro}/S_{BET}
m-Si	15.29	2.57	11.48	0.0012	0.06	6.8	22.39%
np-Si-3	21.90	3.04	16.93	0.0014	0.11	6.7	17.96%
np-Si-5	41.81	11.87	26.95	0.0051	0.12	5.5	44.04%
np-Si-7	30.87	6.28	22.41	0.0031	0.11	6.1	28.02%

[a)] S_{micro} and [b)] S_{meso} are the surface areas of the micropores and mesopores, respectively; [c)] V_{micro} and [d)] V_{meso} are the volumes of the micropores and mesopores, respectively.

Table S2. Comparison of the electrochemical performance of the as-prepared samples with other Si anode materials for lithium-ion battery.

Samples	Method	Tests done at/Initial discharge specific capacity	Cycling performance: Tests done at/Cycle number/Specific capacity	Ref.
3DNP Si	Chemical dealloying	1.8 A g^{-1} /~3550 mA h g^{-1}	1.8 A g^{-1}/1500/1000 mA h g^{-1}	1
nSi	Electrochemical alloying/dealloying	0.6 A g^{-1} /3342 mA h g^{-1}	0.6 A g^{-1}/400/699 mA h g^{-1}	2
NP-Si	Chemical dealloying	0.2 C /~3400 mA h g^{-1}	1.0 C/100/2100 mA h g^{-1}	3
Porous Si	Electrochemical alloying/dealloying	0.2 A g^{-1} /3343 mA h g^{-1}	1.0 A g^{-1}/500/1383 mA h g^{-1}	4
Porous Si	Chemical dealloying	0.1 A g^{-1} /3450 mA h g^{-1}	0.1 A g^{-1}/258/1368 mA h g^{-1}	5
Cu-coated porous Si	Chemical dealloying	0.2 A g^{-1} /1925 mA h g^{-1}	0.1 A g^{-1}/150/1651 mA h g^{-1}	6
NP-Si	Vapor dealloying	0.2 A g^{-1} /3412 mA h g^{-1}	1.0 A g^{-1}/400/1180 mA h g^{-1}	7
MPSi	Chemical dealloying	0.1 A g^{-1} /2882 mA h g^{-1}	1.0 A g^{-1}/200/1846 mA h g^{-1}	8
Nano Si	Electrochemical alloying/dealloying	1.0 A g^{-1} /3230 mA h g^{-1}	3.0 A g^{-1}/300/1430 mA h g^{-1}	9
2DSi	Vapor dealloying	0.2 A g^{-1} /2578 mA h g^{-1}	1.0 A g^{-1}/700/1514 mA h g^{-1}	10
Nanoporous Si	Electrochemical alloying/dealloying	1 A g^{-1} /3276 mA h g^{-1}	1.0 A g^{-1}/800/1309 mA h g^{-1} 5.0 A g^{-1}/1000/1012 mA h g^{-1} 7.0 A g^{-1}/1000/823 mA h g^{-1}	**This work**

Table S3. The calculated impedance parameters of (R_e, R_{ct}, σ, and D_{Li^+}) the m-Si and np-Si-5 electrodes.

Electrodes	R_e (Ω)	R_{ct} (Ω)	σ (Ω $s^{-1/2}$)	D_{Li^+} (cm^2 s^{-1})
m-Si	17.9	237.6	25.5	1.92×10^{-12}
np-Si-5	7.3	94.9	7.3	2.33×10^{-11}

References

1 T. Wada, T. Ichitsubo, K. Yubuta, H. Segawa, H. Yoshida and H. Kato, *Nano Lett.*, 2014, **14**, 4505-4510.

2 Q. Ma, Z. Zhao, Y. Zhao, H. Xie, P. Xing, D. Wang and H. Yin, *Energy Storage Mater.*, 2021, **34**, 768-777.

3 T. Wada, J. Yamada and H. Kato, *J. Power Sources*, 2016, **306**, 8-16.

4 C. Zhang, Q. Ma, M. Cai, Z. Zhao, H. Xie, Z. Ning, D. Wang and H. Yin, *Waste Manag*, 2021, **135**, 182-189.

5 Z. Jiang, C. Li, S. Hao, K. Zhu and P. Zhang, *Electrochim. Acta*, 2014, **115**, 393-398.

6 C. Li, P. Zhang and Z. Jiang, *Electrochim. Acta*, 2015, **161**, 408-412.

7 Y. An, H. Fei, G. Zeng, L. Ci, S. Xiong, J. Feng and Y. Qian, *ACS Nano*, 2018, **12**, 4993-5002.

8 W. Cao, K. Han, M. Chen, H. Ye and S. Sang, *Electrochim. Acta*, 2019, **320**, 134613-134621.

9 Y. Yuan, W. Xiao, Z. Wang, D. J. Fray and X. Jin, *Angew. Chem., Int. Ed.*, 2018, **57**, 15743-15748.

10 Y. An, Y. Tian, C. Wei, H. Jiang, B. Xi, S. Xiong, J. Feng and Y. Qian, *ACS Nano*, 2019, **13**, 13690-13701.